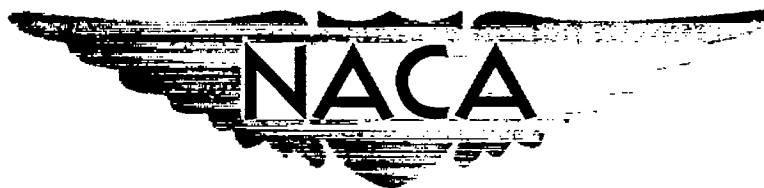


~~CONFIDENTIAL~~

Copy  
RM E51A25

EAR 7 1951



# RESEARCH MEMORANDUM

INVESTIGATION OF ALTITUDE IGNITION, ACCELERATION

AND STEADY-STATE OPERATION WITH SINGLE

COMBUSTOR OF J47 TURBOJET ENGINE

By William P. Cook and Helmut F. Butze

~~CLASSIFICATION CHANGED~~  
Lewis Flight Propulsion Laboratory  
Cleveland, Ohio

UNCLASSIFIED

To

FOR REFERENCE

By authority of

Date

AMT 12-19-57

CLASSIFIED DOCUMENT

NOT TO BE TAKEN FROM THIS ROOM

This document contains classified information affecting the National Defense of the United States within the meaning of the Espionage Act, USC 50:31 and 32. Its transmission or the revelation of its contents in any manner to an unauthorized person is prohibited by law.

Information so classified may be imparted only to persons in the military and naval services of the United States, appropriate civilian officers and employees of the Federal Government who have a legitimate interest therein, and to United States citizens of known loyalty and discretion who of necessity must be informed thereof.

## NATIONAL ADVISORY COMMITTEE FOR AERONAUTICS

WASHINGTON

March 5, 1951

~~CONFIDENTIAL~~

NACA LIBRARY  
LAWRENCE AERONAUTICAL LABORATORY  
LAWRENCE, MISSOURI

NACA RM E51A25



NATIONAL ADVISORY COMMITTEE FOR AERONAUTICS

RESEARCH MEMORANDUM

INVESTIGATION OF ALTITUDE IGNITION, ACCELERATION,

AND STEADY-STATE OPERATION WITH SINGLE

COMBUSTOR OF J47 TURBOJET ENGINE

By William P. Cook and Helmut F. Butze

SUMMARY

An investigation was conducted with a single combustor from a J47 turbojet engine using weathered aviation gasoline and several spark-plug modifications to determine altitude ignition, acceleration, and steady-state operating characteristics.

Satisfactory ignition was obtained with two modifications of the original opposite-polarity spark plug up to and including an altitude of 40,000 feet at conditions simulating equilibrium windmilling of the engine at a flight speed of 400 miles per hour. At a simulated altitude of 30,000 feet, satisfactory ignition was obtained over a range of simulated engine speeds. No significant effect of fuel temperature on ignition limits was observed over a range of fuel temperatures from 80° to -52° F.

At an altitude of 30,000 feet, the excess temperature rise available for acceleration at low engine speeds was limited by the ability of the combustor to produce temperature rise, whereas at high engine speeds the maximum allowable turbine-inlet temperature became the restricting factor.

Altitude operational limits increased from about 51,500 feet at 55 percent of rated engine speed to about 64,500 feet at 85 percent of rated speed. Combustion efficiencies varied from 39.0 to 92.6 percent over the range investigated and decreased with a decrease in engine speed and with an increase in altitude; higher efficiencies would have been obtained if lower altitudes had been investigated. Comparisons were made of the combustion efficiencies of weathered aviation gasoline

and MIL-F-5616 fuel at altitudes of 30,000 and 40,000 feet. Combustion efficiencies obtained with MIL-F-5616 fuel were 8 percent higher at rated engine speed and 14 percent lower at 55 percent of rated speed than those obtained with weathered aviation gasoline.

## INTRODUCTION

Experience has shown that the performance of a turbojet combustor is dependent on flight conditions and that poor performance is generally encountered at high altitudes and at low engine speeds. Consequently, a general program to determine the performance characteristics of turbojet combustors under various flight conditions is being conducted at the NACA Lewis laboratory with a view to establishing optimum design criterions. Steady-state characteristics, such as altitude operational limits, combustion efficiency, and pressure drop, of single combustors both of the annular and of the can type have been investigated for different designs and for a number of different fuels (for example, references 1 to 4). Altitude ignition and acceleration are, of course, of great importance for multiengine planes having one or more engines temporarily inoperative or for single-engine fighters incurring blow-out at high altitudes. A study of the ignition characteristics of several fuels in a single can-type combustor is presented in reference 5 and a wind-tunnel investigation of altitude starting and acceleration characteristics of the J47 engine is reported in reference 6.

In addition to such factors as inertia of the rotating parts and decreased air mass flow at altitude, an important factor affecting acceleration of a turbojet plane is the temperature rise produced by the combustor in excess of that required to maintain the engine at steady-state operation for a given flight condition. This excess temperature rise available for acceleration is normally limited for two reasons: (1) Flame blow-out may occur as the result of over-rich fuel-air ratios; or (2) allowable turbine-inlet temperatures may be exceeded.

The investigation reported herein was conducted to determine the altitude ignition and acceleration characteristics of a single J47 combustor. Additional data were obtained to evaluate the altitude operational limits, combustion efficiency, and total-pressure losses of the combustor. Ignition limits were determined at an altitude of 30,000 feet and at engine rotational speeds below and above equilibrium windmilling speeds for simulated flight speeds of 400 and 354 miles per hour, respectively. Additional ignition-limit tests were made over a range of altitudes for a simulated flight speed of 400 miles per hour and an engine speed equivalent to equilibrium windmilling speed. Acceleration

2017

characteristics were determined at a 30,000-foot simulated altitude over a wide range of engine rotational speeds (12.7- to 88.6-percent rated engine speed) at a simulated flight speed of 400 miles per hour at and below equilibrium windmilling speed and 354 miles per hour above equilibrium windmilling speed. All tests, including those for altitude operational limit and combustion efficiency, were made with weathered aviation gasoline that corresponded to MIL-F-5572, grade 115/145 fuel, from which 15 percent of the more volatile constituents had been removed to simulate altitude vaporization losses. Limited tests for comparisons were made with MIL-F-5616, a kerosene-type fuel that is the design fuel for the J47 combustor.

#### APPARATUS

The installation of the J47 combustor photographically shown in figure 1 followed typical NACA procedure (reference 1). A diagrammatic sketch of the complete experimental setup showing the location of control equipment as well as the location of instrumentation planes is presented in figure 2. Instead of an electric preheater, a gasoline-fired preheater (reference 4) was used. A detailed cross-sectional sketch of the combustor (including inlet and outlet diffusers having the same contour and dimensions as the corresponding engine parts) is shown in figure 3. Fuel was supplied to the combustor by means of a duplex-type spray nozzle; the rate of fuel flow was controlled by a manual valve located downstream of a calibrated rotameter and a high-pressure pump and separated from the nozzle by approximately 10 feet of 3/8-inch outside-diameter tubing. Ignition was effected by means of one of three different types of spark plug, a description of which follows.

Plug A. - Two single electrodes of opposite polarity entered from diametrically opposed holes in the combustion chamber and formed a 1/4-inch spark gap at the center line of the combustor,  $3\frac{1}{2}$  inches from the domed inlet end (fig. 3). This plug, made at the Lewis laboratory according to the manufacturer's recommendation, utilized most of the machined bodies of production plugs and had special porcelain insulators and center electrodes of 1/8-inch inside-diameter alloy tubing through which was passed cooling air from the combustor-inlet diffuser. Plug A was used for most of the ignition tests and all other tests reported herein.

Plug B. - This plug was an experimental, opposite-polarity spark plug supplied by the manufacturer. The electrodes, instead of entering from opposite sides of the combustor, were about 110° apart and formed a 1/4-inch gap at the same position as plug A. The cooling air

for this plug entered through a 1/2-inch hole in the skirt of the plug; the hole was located between the combustor housing and the liner and faced upstream. The air entering the plug through this 1/2-inch hole then divided, a portion blanketing the exposed porcelain and the remainder passing down the hollow center of the electrode tubing (0.146-in. O.D.) and thence into the combustion chamber.

Plug C. - This plug was the same as spark plug B except that the 1/2-inch air holes in the skirt of the plug were reduced to a 1/4-inch diameter.

A standard ignition coil supplied by the manufacturer was used in conjunction with all three spark plugs.

#### INSTRUMENTATION

Air flow and fuel flow to the combustor were metered by a standard A.S.M.E. thin-plate orifice and by calibrated rotameters, respectively. Temperatures and pressures of the inlet air were measured by two single-junction iron-constantan thermocouples and by three, three-point total-pressure rakes and one static-pressure tap, respectively, located at plane A-A (fig. 2) and arranged as shown in figure 4.

Temperatures of the combustor-exit gases were measured by seven banks of five-junction chromel-alumel thermocouple rakes located at plane B-B (fig. 2), corresponding approximately to the position of the turbine blades in the complete engine. Combustor-exit gas total pressures were measured at plane C-C (fig. 2) by seven banks of five-point pressure rakes; a wall static-pressure measurement was made at the same plane. All total-pressure and temperature probes (fig. 4) were located at the centers of equal areas, resulting in one pressure and one temperature reading for each 0.916 square inch of cross-sectional area. Fuel temperatures were measured by a single-junction iron-constantan thermocouple in the fuel line immediately ahead of the combustor.

#### PROCEDURE

In order to investigate altitude ignition and acceleration, it is necessary to determine the engine operating conditions that would be encountered at the sudden opening of inlet-air gates to a parasitic-type engine at a given altitude and flight speed. Transient inlet-air conditions below equilibrium windmilling speed were calculated for an altitude of 30,000 feet and a flight speed of 400 miles per hour (using a derivation included in the appendix) and are given in

figure 5(a). Combustor operating conditions at equilibrium windmilling (2100 rpm or 26.6 percent of rated speed) and for rotational speeds between windmilling and rated speed (7900 rpm) were determined from previous NACA investigations (reference 7) and are shown in figure 5(b).

For the ignition tests, inlet-air conditions were adjusted to simulate a given flight condition, the spark plug was energized, and the fuel flow turned on. Only ignition occurring within 45 seconds after the opening of the fuel valve, as indicated by a sudden rise in the combustor-outlet temperature, was considered satisfactory. Various fuel-flow rates were investigated. Data were taken at various altitudes at equilibrium windmilling conditions with fuel temperatures varying between 70° and 80° F, (normal test-cell conditions) and with the fuel maintained at the temperature of the ambient air at the simulated altitude. Additional ignition data were taken at an altitude of 30,000 feet for engine rotational speeds above and below equilibrium windmilling speed and with a fuel temperature of 70° to 80° F.

Acceleration tests were conducted by two methods, a slow-throttle and a rapid-throttle advance. For the slow-throttle advance, inlet-air conditions and fuel-flow rate were adjusted to simulate a given altitude and rotational speed. Then, with inlet-air conditions held constant, the fuel flow was slowly increased until blow-out or excessive temperatures (above 1700° F, considered by the manufacturer to be the limiting turbine-inlet temperature) were encountered. The difference between the initial combustor-outlet temperature, required to maintain steady-state engine operation, and the final outlet temperature was taken as a measure of the ability of the combustor to produce acceleration. For tests at or below equilibrium windmilling speeds, the entire temperature rise across the combustor may be considered to be available for producing acceleration. For the rapid-throttle advance tests, the inlet-air conditions and fuel-flow rates were adjusted as before; the fuel flow was then increased in 3 seconds to a value registered on the rotameter equal to three-fourths of the maximum fuel-flow rate obtained with slow-throttle advance. If flame blow-out did not occur, the procedure was repeated to successively higher fuel-flow rates. Combustor-outlet temperatures attained after stabilization of combustion were used in the rapid-throttle tests because of the difficulty in determining with thermocouples the instantaneous average temperature at the end of the 3-second throttle advance.

Altitude operational limits and combustion efficiencies at various simulated-flight conditions were determined. Inlet-air temperature, pressure, and mass flow were set for the particular flight condition investigated and the fuel flow adjusted to give the required combustor temperature rise. Conditions at which the required temperature rise

could not be attained were considered to be in the inoperable range of the engine. All data were taken with the spark plug de-energized.

In order to simulate more closely operation at altitude, a limited number of tests was repeated with the fuel at altitude ambient-air temperature rather than at room temperature. The test fuel used during the greatest part of the investigation was weathered aviation gasoline, corresponding to MIL-F-5572, grade 115/145 fuel, from which 15 percent of the more volatile constituents had been removed to simulate altitude vaporization losses. Comparison tests were made with MIL-F-5616 fuel, the design fuel for the J47 combustor. Physical data for the two fuels are presented in table I.

Combustor inlet-air and outlet-gas total pressure were also recorded for the determination of the pressure drop through the combustor.

#### Calculations

Combustion efficiency, as used herein, is arbitrarily defined as the ratio of the increase in enthalpy of the air and combustion products to the heat available in the fuel, and was calculated as described in reference 8. Thermocouple indications were taken as true values of total temperature with no correction for radiation or stagnation effects. In order to record combustor pressure losses on a dimensionless basis, the ratio of the pressure loss to a reference dynamic pressure was used. The reference dynamic pressure was computed for each experimental condition from the air flow through the combustor, the density at the combustor inlet, and the maximum cross-sectional area of the combustor housing.

### RESULTS AND DISCUSSION

#### Ignition

The results of the ignition tests are shown in figure 6 for the J47 combustor operating with weathered aviation gasoline (fuel temperature 70° to 80° F) and with spark plug A. With inlet-air conditions to the combustor simulating a flight speed of 400 miles per hour and the engine windmilling at 26.6 percent of rated speed (the equilibrium windmilling speed for this flight speed), ignition was obtained up to and including an altitude of 40,000 feet. The time required for ignition to occur increased from 3 seconds at 25,000 feet to 15 seconds at 35,000 feet and to 45 seconds at 40,000 feet. No ignition was obtained at 45,000 feet with any fuel flow applied. The range of fuel flows over which ignition occurred decreased significantly as the altitude

increased. At 30,000 feet, a variation of about  $\pm 10$  percent from a starting fuel-air ratio of approximately 0.015 was possible; whereas at 40,000 feet, the allowable variation from this fuel-air ratio was less than  $\pm 2$  percent.

At a simulated altitude of 30,000 feet and a flight speed of 400 miles per hour, satisfactory ignition was obtained with spark plug A at windmilling conditions ranging from 12.7 to 26.6 percent of rated engine speed. At this same altitude and a flight speed of 354 miles per hour, ignition was satisfactory at steady-state conditions ranging from 26.6 to 88.6 percent of rated speed. No difference in results was obtained with the fuel at room temperature and with the fuel cooled to altitude ambient-air temperature.

With spark plug B, ignition was obtained only up to and including 30,000 feet for conditions simulating equilibrium windmilling at a flight speed of 400 miles per hour. With spark plug C, the results were the same as with plug A; thus the reduced flow of cooling air to the electrodes served to improve the ignition performance of plug C over that of plug B.

#### Acceleration

The combustor temperature rise obtained with a slow-throttle advance is shown in figure 7 as a function of fuel-air ratio for various windmilling and steady-state operating conditions at an altitude of 30,000 feet. For the range of speeds investigated, from 15.2 to 63.3 percent of rated engine speed, the maximum obtainable temperature rise is limited by blow-out.

In order to show more clearly the effect of increasing engine speed, values of maximum obtainable temperature rise for both slow- and rapid-throttle advance at an altitude of 30,000 feet have been plotted in figure 8 as a function of engine speed. Maximum-temperature-rise values for the slow-throttle advance were taken from the blow-out points shown in figure 7; values for the rapid-throttle advance were obtained from the temperatures attained after stabilization of combustion. Rapid-throttle advance, as previously explained, consisted of a 3-second advance of the fuel throttle to the maximum opening possible without resultant blow-out. Also shown in figure 8 are the temperature rise required for steady-state operation of the engine at this altitude and flight speed (as calculated from the curves in fig. 5(b)) and the maximum allowable temperature rise based on a limiting turbine-inlet temperature of  $1700^{\circ}\text{F}$ .



With the rapid-throttle advance, the maximum obtainable temperature rise increased from  $880^{\circ}\text{F}$  at about 32.5 percent of rated speed to  $1500^{\circ}\text{F}$  at 75 percent of rated speed. Further temperature increases at engine speeds above 75 percent of rated speed were prohibited by excessive combustor-outlet temperatures. With slow-throttle advance, at conditions simulating steady-state engine operation at a flight speed of 354 miles per hour, the maximum obtainable temperature rise increased from  $1040^{\circ}\text{F}$  at about 31.5 percent of rated speed to  $1550^{\circ}\text{F}$  at about 66.5 percent of rated speed and again was limited by the excessive combustor-outlet temperatures encountered at the higher engine speeds. At windmilling conditions (26.6 percent of rated engine speed and below), the maximum temperature rise that could be obtained with slow-throttle advance decreased from  $1590^{\circ}\text{F}$  at 15.2 percent of rated speed to  $720^{\circ}\text{F}$  at 26.6 percent of rated speed.

The excess temperature rise available for acceleration, that is, the difference between the maximum temperature rise obtainable and the temperature rise required for steady-state engine operation, is shown in figure 9 for both slow- and rapid-throttle advance. The solid curve with negative slope represents the difference between allowable temperature rise (based on a limiting turbine-inlet temperature of  $1700^{\circ}\text{F}$ ) and the temperature rise required to maintain steady-state engine operation. Thus, it is evident that in the low-speed range, the excess temperature rise available for combustion is limited by the ability of the combustor to provide temperature rise; whereas at the higher engine speeds, the temperature rise available for acceleration is limited by the maximum allowable combustor-outlet temperature because the combustor is capable of producing outlet temperatures exceeding  $1700^{\circ}\text{F}$ . The dashed curve in figure 9 shows calculated values of excess temperature rise available for acceleration at simulated sea-level flight conditions, again based on a limiting combustor-outlet temperature of  $1700^{\circ}\text{F}$ . Low-altitude conditions are favorable for combustion, and experience has shown that combustor-outlet temperatures in excess of  $1700^{\circ}\text{F}$  can be attained at these conditions. Thus, at sea-level conditions, the temperature rise available for acceleration is limited throughout the entire range of engine speeds by the maximum allowable turbine-inlet temperature of  $1700^{\circ}\text{F}$ .

A comparison of the sea-level and the experimental 30,000-foot temperature-rise curves of figure 9 shows that, in the low-speed range, the excess temperature rise available for acceleration is much greater at sea level than at altitude, a factor that contributes toward the lower rate of acceleration encountered at altitude. Another important factor, of course, is the decrease in air mass flow rate at high altitudes while the inertia of the rotating parts remains constant as was previously mentioned.

### Altitude Operational Limits

The altitude operational limits of the J47 combustor operating with weathered aviation gasoline at a flight Mach number of 0.52 are presented in figure 10. The altitude-limit curve was established by interpolation between data points obtained at two simulated altitudes 5000 feet apart: one at which the required temperature rise was obtained and one at which it was not obtainable. The manner of interpolation was based upon observation of the combustor during the test. The determination of the altitude limits was restricted to engine rotational speeds between 55 and 85 percent of rated speed because at the low end of the speed range the required low combustor inlet-air temperatures were limited by the laboratory facilities; whereas at the high end of the speed range the ability of the thermocouples to withstand the high combustor-outlet temperatures required was the restricting factor. Figure 10 shows that the altitude operational limits increased from 51,500 feet at 55 percent of rated engine speed to 64,550 feet at 85 percent of rated speed. With the slow-throttle advance used in this phase of the investigation, no flame blow-out was encountered.

### Combustion Efficiency

Combustion efficiencies obtained with the J47 combustor operated at various simulated altitudes and engine speeds with room-temperature weathered aviation gasoline are shown in figure 10. The combustion efficiencies varied from 39.0 to 92.6 percent at the conditions investigated and followed the general trends typical of gas-turbine combustors, decreasing with a decrease in engine speed and with an increase in altitude. The constant combustion-efficiency lines shown in figure 10 were obtained by interpolation between the values of efficiency obtained at the test points. Operation of the combustor with fuel at altitude ambient-air temperature resulted in random variations in combustion efficiency of 0 to about 2 percent from those shown in figure 10; thus, for the conditions investigated, fuel temperature had little effect on combustion efficiency.

A comparison of the combustion efficiencies obtained with MIL-F-5616 fuel, the design fuel for the J47 engine, and with weathered aviation gasoline at various engine speeds and at altitudes of 30,000 and 40,000 feet is shown in figure 11. At both altitudes and at rated engine speed, combustion efficiencies obtained with MIL-F-5616 fuel were about 8 percent higher than those obtained with weathered aviation gasoline; at 55 percent of rated engine speed, however, operation with MIL-F-5616 fuel resulted in a decrease of about 14 percent in combustion efficiency.

### Pressure Loss

The total-pressure loss across the combustor is shown in figure 12. The ratio of the total-pressure loss to a reference dynamic pressure  $\Delta P/q_r$  is plotted against the ratio of the inlet-air density to the exhaust-gas density  $\rho_1/\rho_2$  and a straight-line correlation was obtained. Figure 12 indicates that the total-pressure loss ratio increased from 12.3 to about 16.1 as the density ratio increased from 1 to 2.6.

### SUMMARY OF RESULTS

From an investigation of the ignition, acceleration, and steady-state operational characteristics of a single combustor of a J47 engine using weathered aviation gasoline with opposite-polarity spark plugs at simulated flight conditions, the following results were obtained:

1. With combustor inlet-air conditions simulating equilibrium windmilling at a flight speed of 400 miles per hour, satisfactory ignition was obtained with spark plug A up to and including 40,000 feet. No significant effect of fuel temperature on ignition was observed over the range of fuel temperatures investigated.
2. At a simulated altitude of 30,000 feet, satisfactory ignition was obtained with spark plug A over a speed range from 12.7 to 26.6 percent of rated engine speed, representing windmilling conditions, and over a range from 31.8 to 88.6 percent of rated speed, representing steady-state operation of the combustor.
3. The altitude ignition limit of the combustor was significantly increased by a reduction in the quantity of cooling air supplied through the electrodes of the experimental spark plug (plug B) furnished by the manufacturer.
4. At an altitude of 30,000 feet, the excess temperature rise available for acceleration at low engine speeds was limited by the ability of the combustor to produce temperature rise, whereas at high engine speeds the maximum allowable turbine-inlet temperature was the restricting factor.
5. The altitude operational limits increased from about 51,500 feet at 55 percent of rated engine speed to about 64,500 feet at 85 percent of rated speed.
6. The combustion efficiencies varied from 39.0 to 92.6 percent, decreasing with a decrease in engine speed and with an increase in

altitude. Higher efficiencies would have been obtained if lower altitudes had been investigated. No significant effect of fuel temperature on combustion efficiency was observed over the range of fuel temperature investigated ( $80^{\circ}$  to  $-52^{\circ}$  F).

7. At altitudes of 30,000 and 40,000 feet the combustion efficiencies obtained with MIL-F-5616 fuel were about 8 percent higher at rated engine speed and 14 percent lower at 55 percent of rated speed than those obtained with weathered aviation gasoline.

8. The pressure-loss ratio increased from 12.3 to 16.1 when the density ratio was raised from 1 to 2.6.

Lewis Flight Propulsion Laboratory,  
National Advisory Committee for Aeronautics,  
Cleveland, Ohio.

mjb

## APPENDIX - CALCULATION OF COMBUSTOR OPERATING CONDITIONS

## Symbols

The following symbols are used in the calculations:

M	Mach number
N	engine rotational speed
P	absolute total pressure
p	absolute static pressure
T	absolute total temperature
t	absolute static temperature
V	true flight speed
$W_a$	mass air flow per unit time through compressor
$\gamma$	specific-heat ratio for air
$\delta$	total pressure divided by standard sea-level pressure
$\theta$	total temperature divided by standard sea-level temperature

## Subscripts:

0	engine inlet (ambient conditions)
1	compressor inlet
2	combustor inlet (compressor outlet)
3	combustor outlet
$y$ $z$	two different engine operating conditions

S.L. sea level

### Combustor-Inlet Conditions with Engine Windmilling

In order to obtain combustor operating data at transitory engine rotational speeds that would be encountered during the opening of the intake gates (closed during nonoperation) of an auxiliary flight turbo-jet installation, corrections were applied to engine equilibrium windmilling data as shown in the following discussion.

Air flow. - In general, the mass flow of air through a compressor is given by

$$\frac{W_{a,z}}{W_{a,y}} = \frac{N_z}{N_y} \frac{P_{1,z}}{P_{1,y}} \frac{t_{1,y}}{t_{1,z}} \quad (1)$$

where the subscripts  $y$  and  $z$  represent two different engine operating conditions. It can also be shown that

$$T_1 = t_1 \left( 1 + \frac{\gamma-1}{2} M_1^2 \right) \quad (2)$$

If no external heat is added to the air during its passage through the engine inlet diffuser,

$$T_1 = T_0 \quad (3)$$

Also, as in equation (2)

$$T_0 = t_0 \left( 1 + \frac{\gamma-1}{2} M_0^2 \right) \quad (4)$$

If the velocity of the air leaving the diffuser and entering the compressor is assumed to be zero (approximate only),

$$T_1 = t_1 \quad (5)$$

From the preceding equations,

$$t_1 = t_0 \left( 1 + \frac{\gamma-1}{2} M_0^2 \right) \quad (6)$$

Thus,

$$\frac{t_{1,y}}{t_{1,z}} = \frac{t_{0,y} \left(1 + \frac{\gamma-1}{2} M_{0,y}^2\right)}{t_{0,z} \left(1 + \frac{\gamma-1}{2} M_{0,z}^2\right)} \quad (7)$$

If both operating conditions are assumed to be for engine operation at the same altitude,

$$t_{0,y} = t_{0,z}$$

and

$$\frac{t_{1,y}}{t_{1,z}} = \left( \frac{1 + \frac{\gamma-1}{2} M_{0,y}^2}{1 + \frac{\gamma-1}{2} M_{0,z}^2} \right) \quad (8)$$

For an assumed diffuser efficiency of 100 percent,

$$p_1 = p_0 \quad (9)$$

Substituting from equation (9) and assuming the diffusion process is isentropic gives

$$\frac{p_1}{p_0} = \frac{p_0}{p_0} = \left( \frac{T_0}{t_0} \right)^{\frac{\gamma}{\gamma-1}} \quad (10)$$

Substituting equation (4) into equation (10) yields

$$\frac{p_1}{p_0} = \left[ \frac{t_0 \left(1 + \frac{\gamma-1}{2} M_0^2\right)}{t_0} \right]^{\frac{\gamma}{\gamma-1}}$$

or

$$p_1 = p_0 \left(1 + \frac{\gamma-1}{2} M_0^2\right)^{\frac{\gamma}{\gamma-1}} \quad (11)$$

Thus

$$\frac{p_{1,z}}{p_{1,y}} = \frac{p_{0,z} \left(1 + \frac{\gamma-1}{2} M_{0,z}^2\right)^{\frac{\gamma}{\gamma-1}}}{p_{0,y} \left(1 + \frac{\gamma-1}{2} M_{0,y}^2\right)^{\frac{\gamma}{\gamma-1}}} \quad (12)$$

applying the same assumptions as applied to equation (8)

$$p_{0,z} = p_{0,y}$$

and

$$\frac{p_{1,z}}{p_{1,y}} = \frac{\left(1 + \frac{\gamma-1}{2} M_{0,z}^2\right)^{\frac{\gamma}{\gamma-1}}}{\left(1 + \frac{\gamma-1}{2} M_{0,y}^2\right)^{\frac{\gamma}{\gamma-1}}} \quad (13)$$

Substituting equations (8) and (13) into equation (1) yields

$$\frac{W_{a,z}}{W_{a,y}} = \frac{N_z}{N_y} \left( \frac{1 + \frac{\gamma-1}{2} M_{0,z}^2}{1 + \frac{\gamma-1}{2} M_{0,y}^2} \right)^{\frac{1}{\gamma-1}} \quad (14)$$

Available operating data included the equilibrium windmilling speeds of the J47 turbojet engine at various flight speeds and the mass air-flow rate through the engine at equilibrium windmilling speeds from 1000 to 2100 rpm. Application of these data to equation (14) enabled the calculation of mass air flows at a flight speed of 400 miles per hour at engine rotational speeds other than the equilibrium windmilling speed.

Inlet pressure. - In addition to equilibrium windmilling speeds at various flight speeds, the operating data of the J47 turbojet engine also included the combustor-inlet total pressures at various equilibrium windmilling speeds. In order to determine combustor-inlet total



pressures at rotational speeds encountered during the opening of the intake gates (that is, transitory windmilling speeds less than the equilibrium windmilling speed corresponding to the particular flight speed), the data were corrected as subsequently shown. Assumed performance data are:

True flight speed	Equilibrium windmilling speed
$V_y$	$N_y$
$V_z$	$N_z$

At the same rotational speed at different flight speeds,

$$(P_2)_{V_z, N_z} = (P_1)_{V_z} - (1 \Delta P_2)_{N_z} \quad (15)$$

$$(P_2)_{V_y, N_z} = (P_1)_{V_y} - (1 \Delta P_2)_{N_z} \quad (16)$$

Subtracting equation (15) from equation (16) yields

$$(P_2)_{V_y, N_z} = (P_2)_{V_z, N_z} + (P_1)_{V_y} - (P_1)_{V_z} \quad (17)$$

Assuming that the diffuser efficiency is 100 percent and the velocity of the air leaving the diffuser is approximately zero yields

$$P_1 = P_0 = p_0 \left( 1 + \frac{\gamma-1}{2} M_0^2 \right)^{\frac{\gamma}{\gamma-1}}$$

By substitution in equation (17),

$$(P_2)_{V_y, N_z} = (P_2)_{V_z, N_z} + p_0 \left[ \left( 1 + \frac{\gamma-1}{2} M_{0,y}^2 \right)^{\frac{\gamma}{\gamma-1}} - \left( 1 + \frac{\gamma-1}{2} M_{0,z}^2 \right)^{\frac{\gamma}{\gamma-1}} \right] \quad (18)$$

or

$$(P_2)_{V_y, N_z} = (P_2)_{V_z, N_z} + p_0 (\text{ram ratio}_{V_y} - \text{ram ratio}_{V_z}) \quad (19)$$

Thus, if the combustor-inlet total pressure is known for an equilibrium windmilling speed at one flight speed, the inlet total pressure can be calculated for the same windmilling speed at another flight speed.

Inlet temperature. - The total temperatures of the air at the combustor inlet for various engine windmilling speeds at altitude conditions were determined by addition of a small temperature rise (3° to 20° F) caused by windmilling of the engine (altitude-wind-tunnel research) to the total temperatures of the air at the compressor inlet (equations (3) and (4)).

#### Combustor-Inlet Conditions for Normal Operation

Combustor operating conditions during normal engine operation at altitude were obtained by adjusting the data from an investigation of a complete engine operated at a simulated Mach number of 0.52. The following values were plotted (fig. 5(b)) against percentage corrected rated engine speed:  $T_2/T_0$ ,  $T_3/T_0$ ,  $W_a/\theta/\delta$ , and  $P_2/\delta$ . These values were then reduced to the uncorrected values at the various altitudes by appropriate treatment with  $\delta$ ,  $\theta$ , or  $T_0$ , and replotted. A working plot of the uncorrected values is not included in this report. Engine-inlet temperature  $T_0$  is given by equation (4), and  $\delta$  and  $\theta$  were determined as

$$\delta = \frac{P_0}{P_{S.L.}} = \frac{1.2 P_0}{P_{S.L.}} \quad (20)$$

$$\theta = \frac{T_0}{t_{S.L.}} = \frac{t_0(1.2)^{\frac{\gamma-1}{\gamma}}}{t_{S.L.}} \quad (21)$$

#### REFERENCES

1. Zettle, Eugene V., and Cook, William P.: Performance Investigation of Can-Type Combustor. I - Instrumentation, Altitude Operational Limits, and Combustion Efficiency. NACA RM E8F17, 1948.
2. Dittrich, Ralph T., and Jackson, Joseph L.: Altitude Performance of AN-F-58 Fuels in J33-A-21 Single Combustor. NACA RM E8L24, 1949.
3. Tischler, Adelbert O., and Dittrich, Ralph T.: Fuel Investigation in a Tubular-Type Combustor of a Turbojet Engine at Simulated Altitude Conditions. NACA RM E7F12, 1947.

4. McCafferty, Richard J.: Effect of Fuels and Fuel-Nozzle Characteristics on Performance of an Annular Combustor at Simulated Altitude Conditions. NACA RM E8C02a, 1948.
5. Payle, Warren D., and Douglass, Howard W.: Investigation of Ignition Characteristics of AN-F-32 and Two AN-F-58 Fuels in Single Can-Type Turbojet Combustor. NACA RM E50H16a, 1950.
6. Golladay, Richard L., and Bloomer, Harry E.: Investigation of Altitude Starting and Acceleration Characteristics of J47 Turbojet Engine. NACA RM E50G07, 1951.
7. Conrad, E. William, and Sobelewski, Adam E.: Altitude-Wind-Tunnel Investigation of J47 Turbojet-Engine Performance. NACA RM E9G09, 1949.
8. Turner, L. Richard, and Bogart, Donald: Constant-Pressure Combustion Charts Including Effects of Diluent Addition. NACA Rep. 937, 1949. (Formerly NACA TNs 1086 and 1655.)

2017

TABLE I - ANALYSIS OF FUELS USED

A.S.T.M. distillation D 86-46, °F	MIL-F-5616	MIL-F-5572 grade 115/145 (weathered)
Initial boiling point	312	120
Percentage evaporated		
10	329	
20	333	
30	338	
40	342	
50	347	210
60	353	
70	361	
80	373	
90	393	
Final boiling point, °F	446	333
Reid vapor pressure, lb/sq in.	0	4.2
Specific gravity at 60° F/60° F	0.791	0.718
TEL, ml/gal	0	5.32
H/C	0.164	0.182
Net heating value, Btu/lb	18,670	18,950

NACA

2017



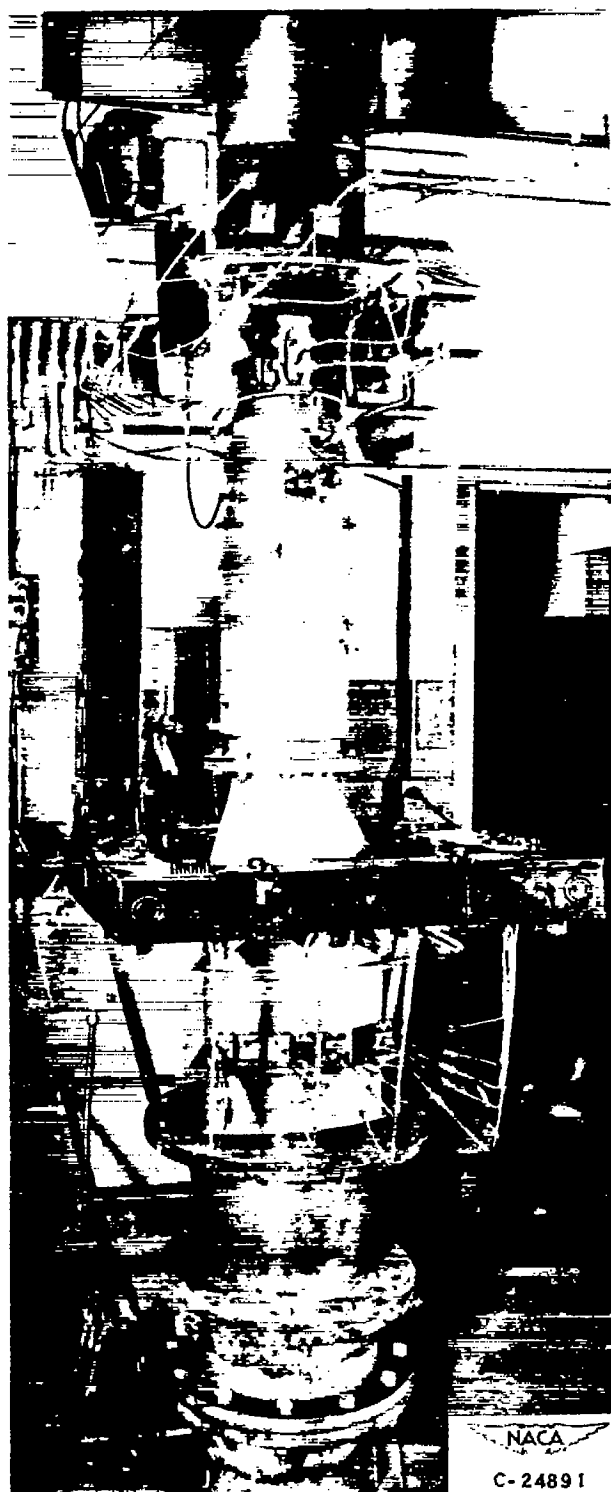


Figure 1. - Single J47 combustor in test setup.



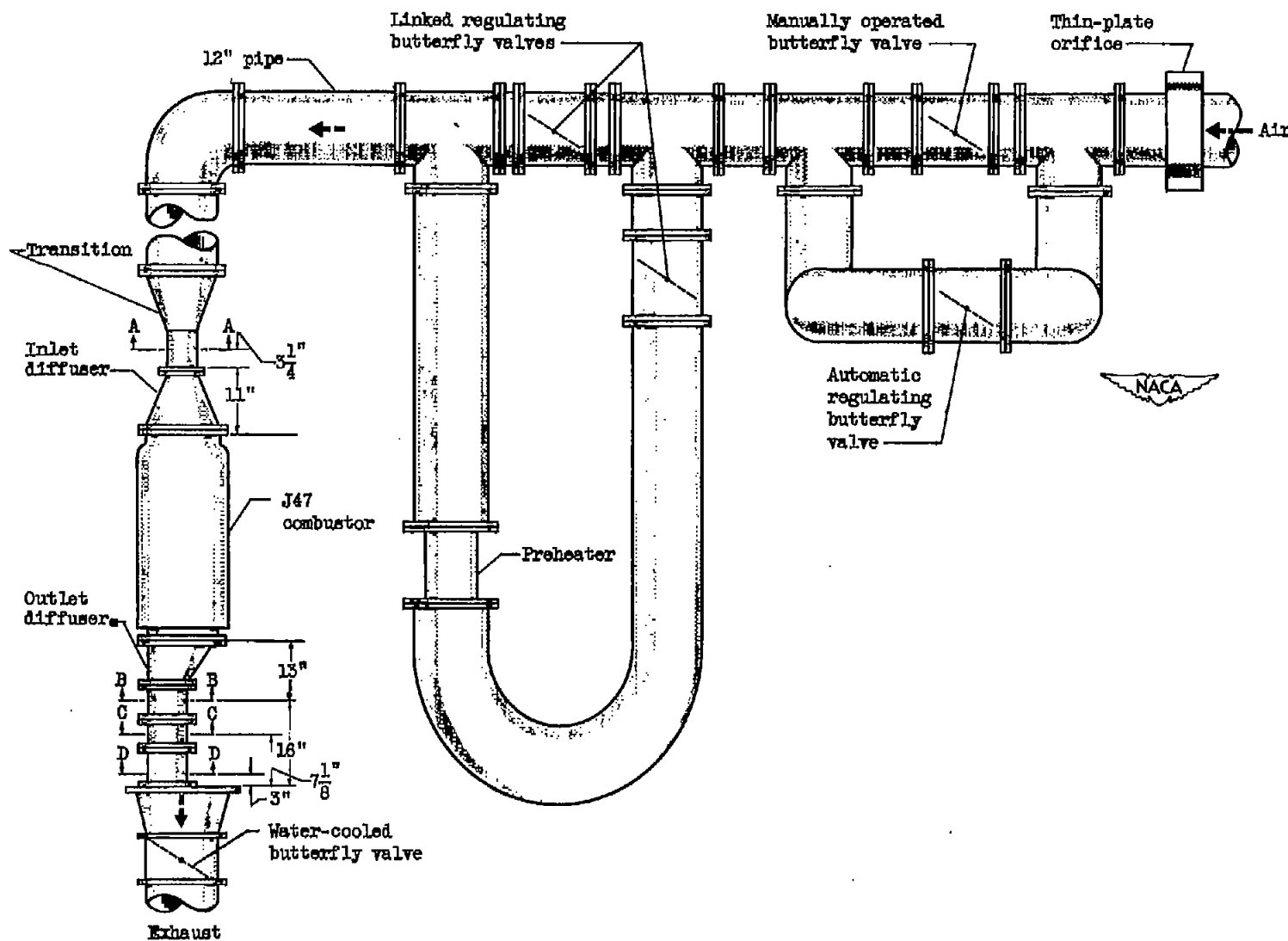


Figure 2. - Diagrammatic sketch of J47 combustor test setup.



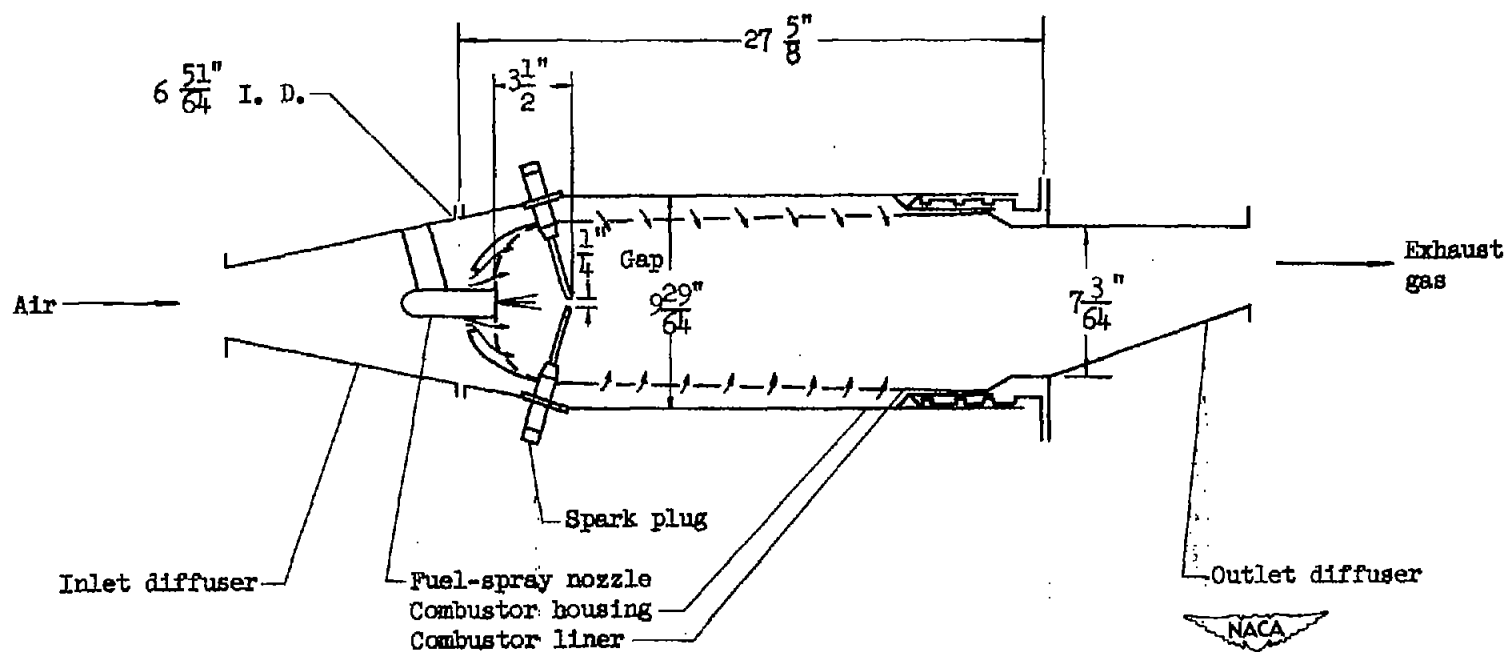
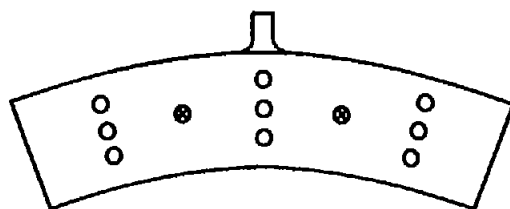
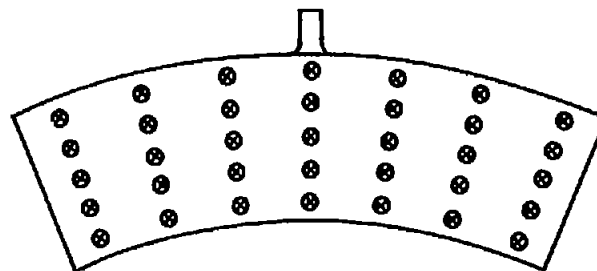


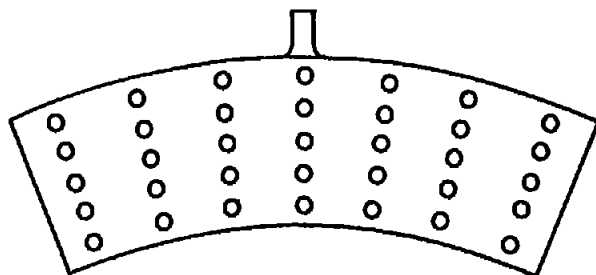
Figure 3. - Sketch of J47 combustor showing relation of various components.



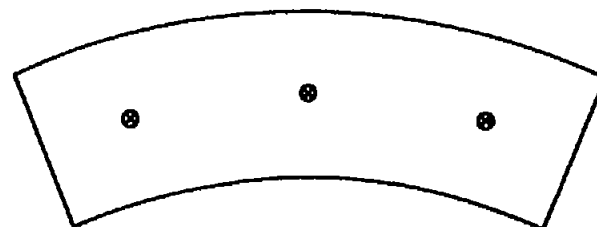
Plane A-A  
(fig. 2)



Plane B-B



Plane C-C

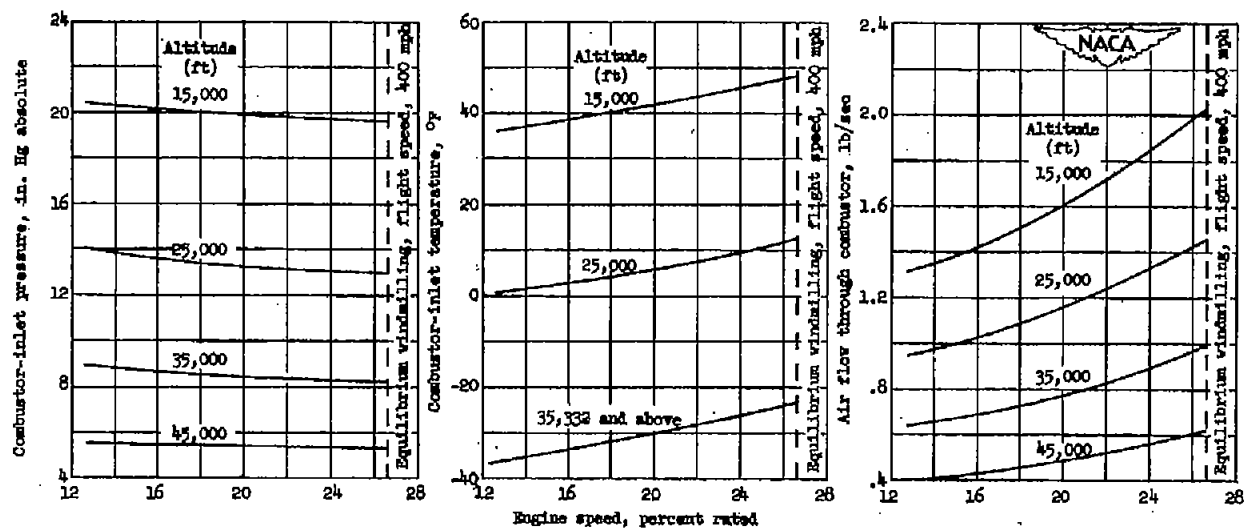


Plane D-D

- Total-pressure tube
- Thermocouple
- ∩ Static-pressure orifice

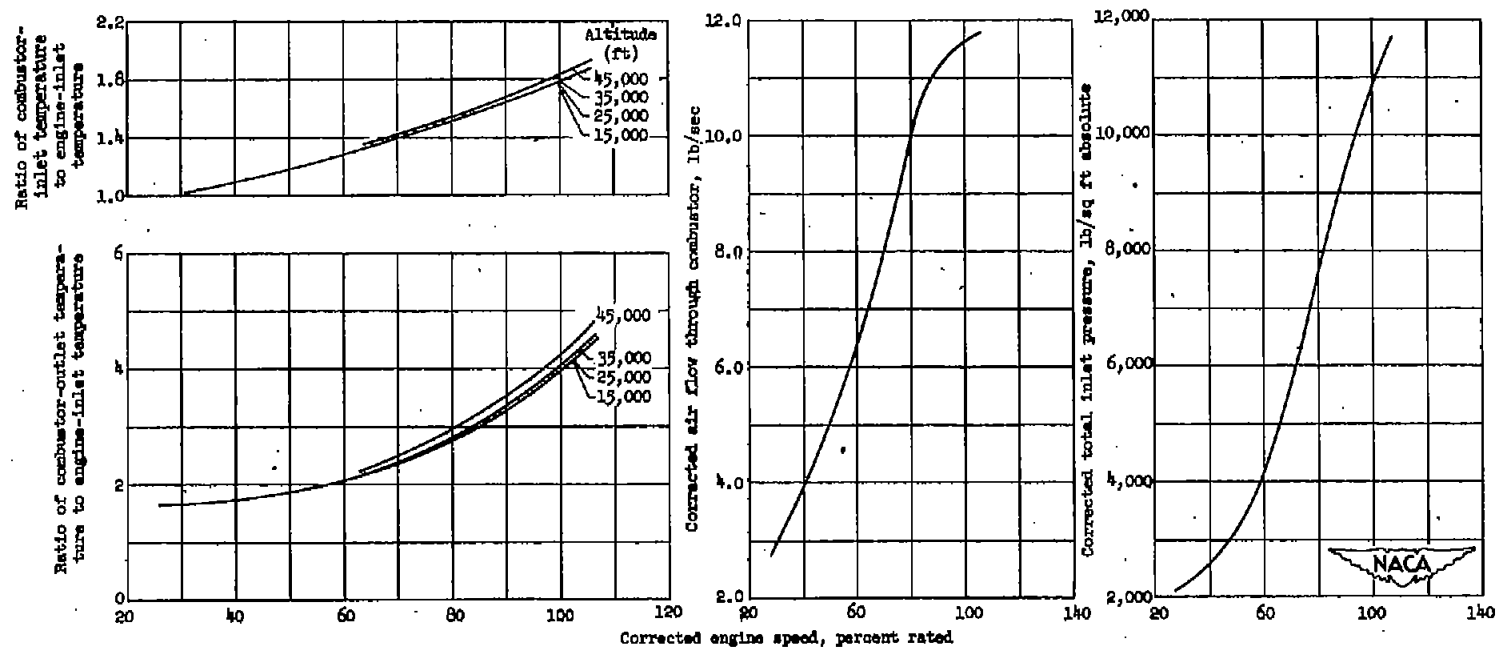


Figure 4. - Location of instruments at several instrumentation planes.



(a) No burning; engine windmilling with flight speed of 400 miles per hour.

Figure 5. - J47 combustor operating conditions. Data calculated from NACA altitude-wind-tunnel investigation (reference 7) by method given in appendix.



(b) . With burning; flight Mach number, 0.52.

Figure 5. - Concluded. J47 combustor operating conditions. Data calculated from NACA altitude-wind-tunnel investigation (reference 7) by method given in appendix.

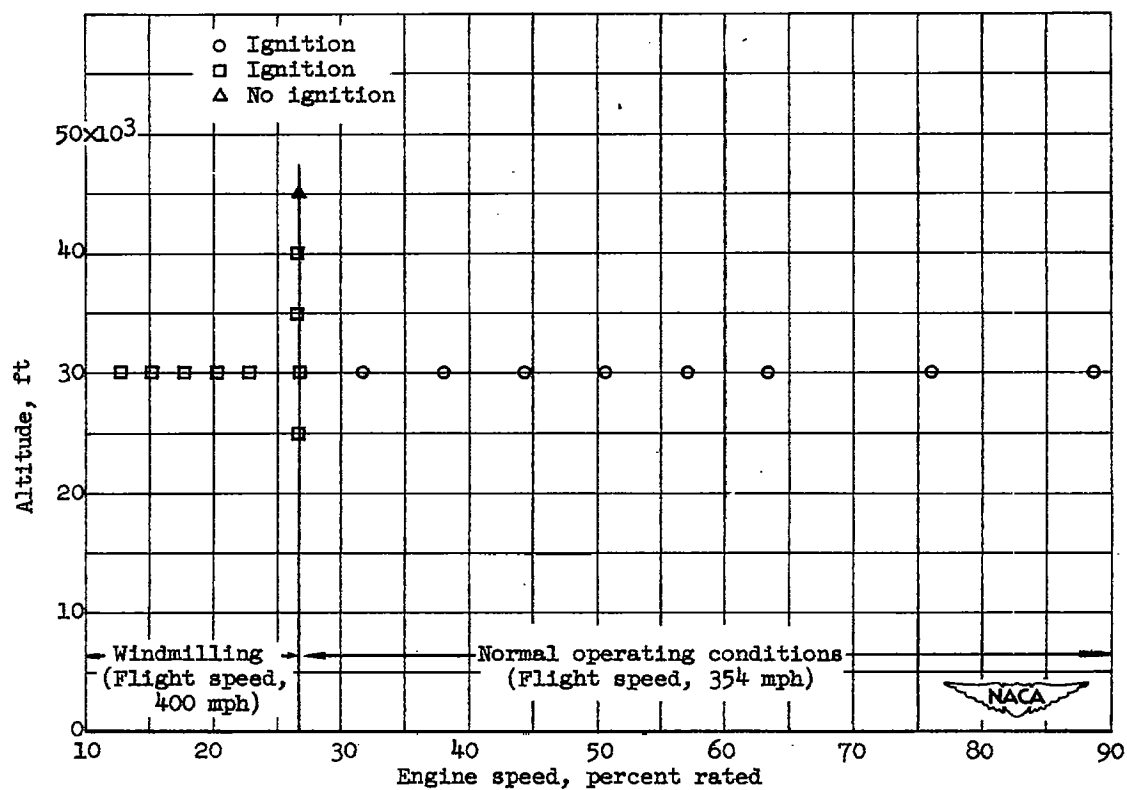
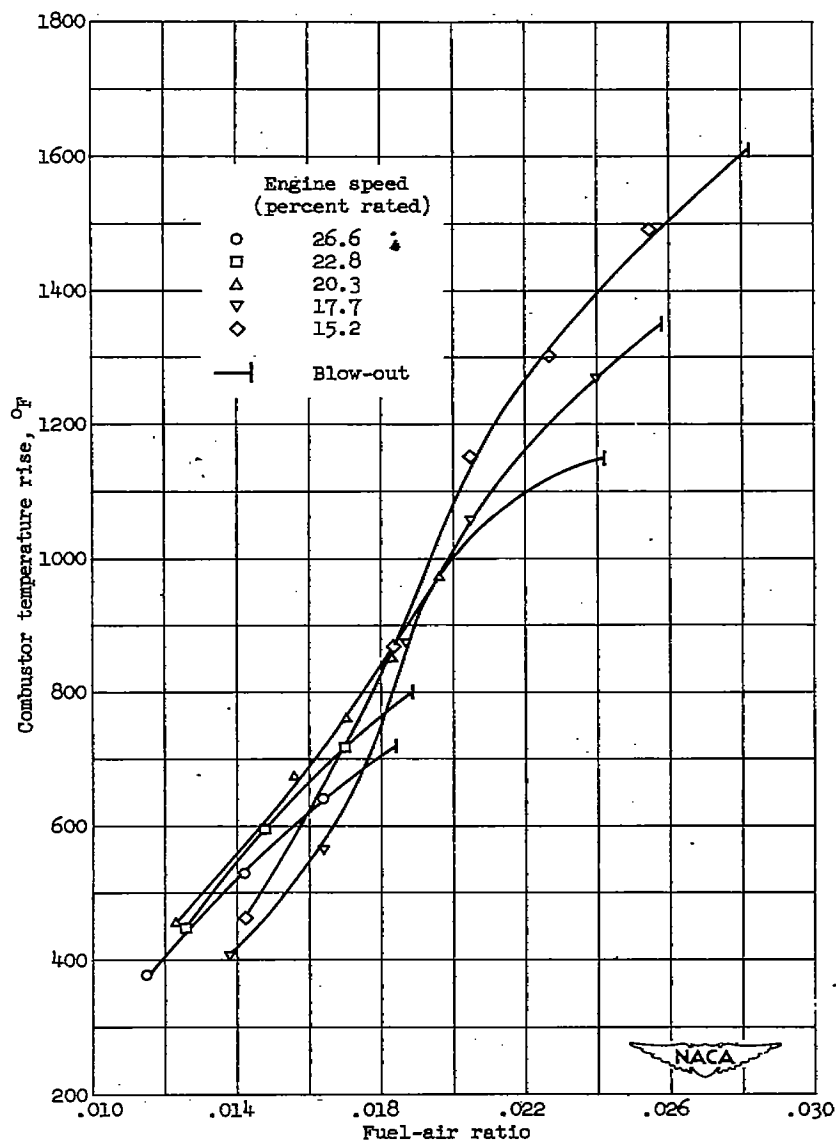
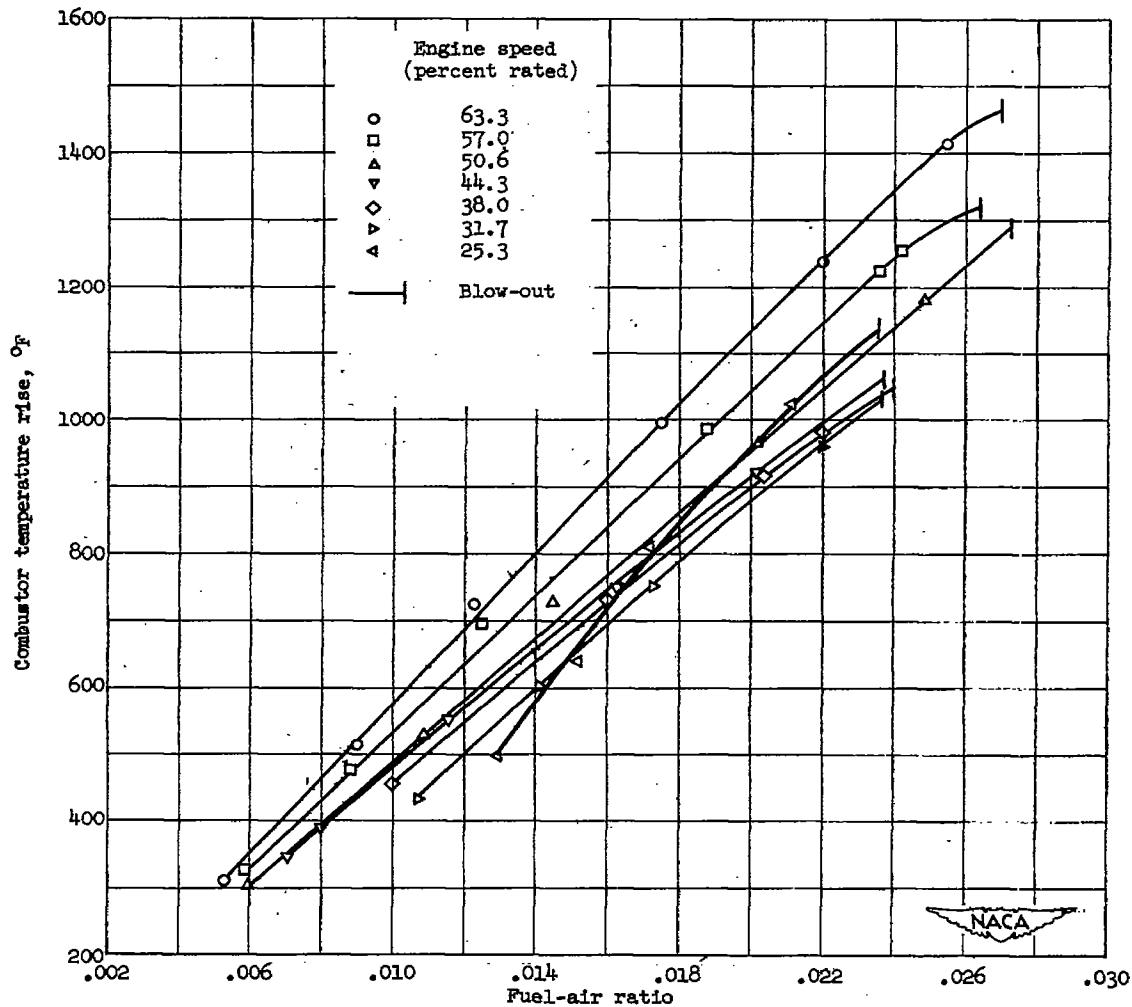


Figure 6. - Altitude-ignition trials with fuel MIL-F-5572, grade 115/145 (weathered).



(a) Flight speed 400 miles per hour and engine windmilling at speeds up to 26.6 percent of rated speed (equilibrium windmill speed at 400 mph).

Figure 7. - Temperature rise obtainable with various fuel-air ratios in J47 single combustor at conditions simulating altitude of 30,000 feet. Fuel, MIL-F-5572, grade 115/145 (weathered).



(b) Engine speeds of 25.3 percent rated and higher; flight speed, 354 miles per hour.

Figure 7. - Concluded. Temperature rise obtainable with various fuel-air ratios in J47 single combustor at conditions simulating altitude of 30,000 feet. Fuel, MIL-F-5572, grade 115/145 (weathered).

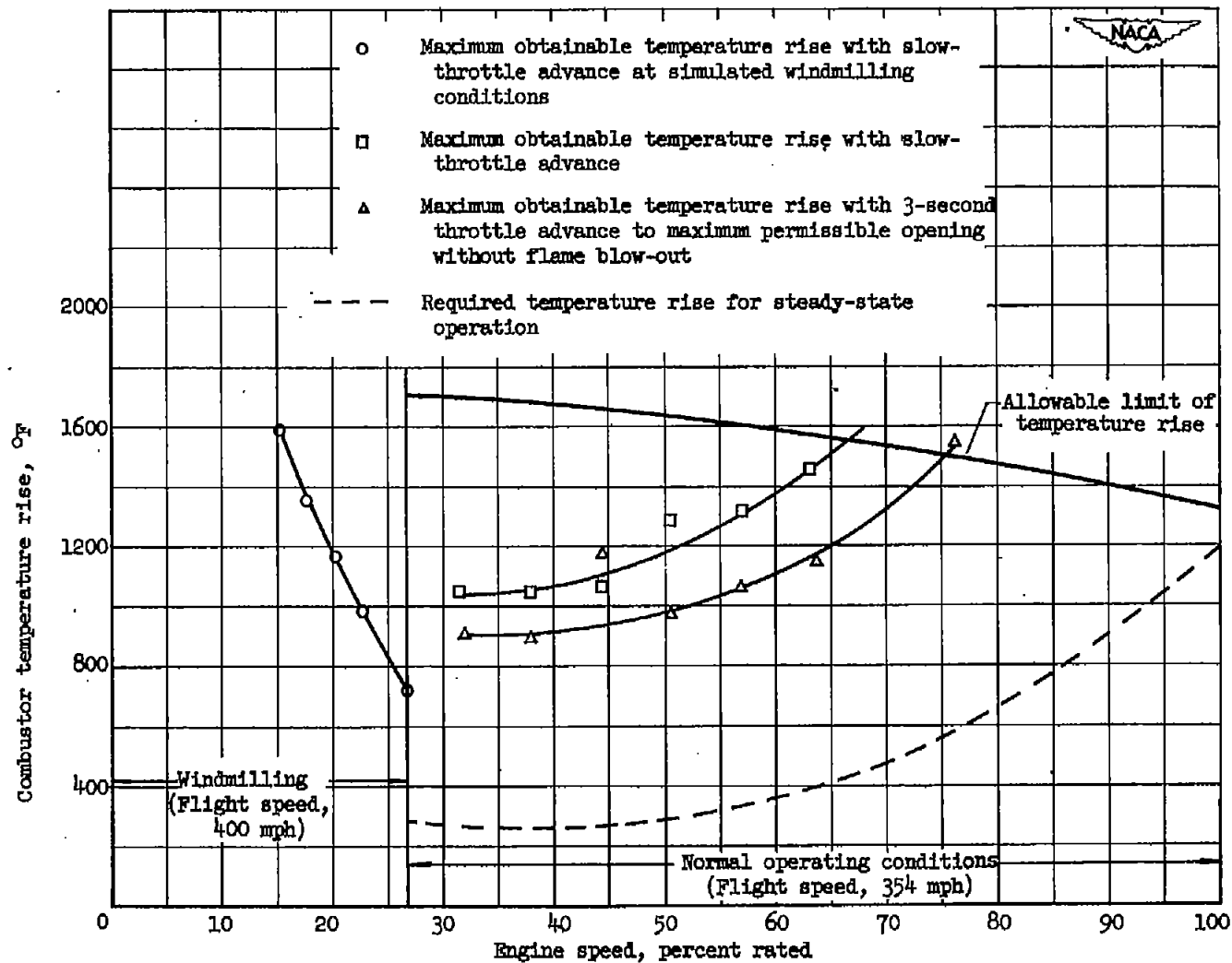


Figure 8. - Values of temperature rise required and obtainable in J47 single combustor over range of engine speeds at conditions simulating altitude at 30,000 feet. Fuel, MIL-F-5572, grade 115/145 (weathered).



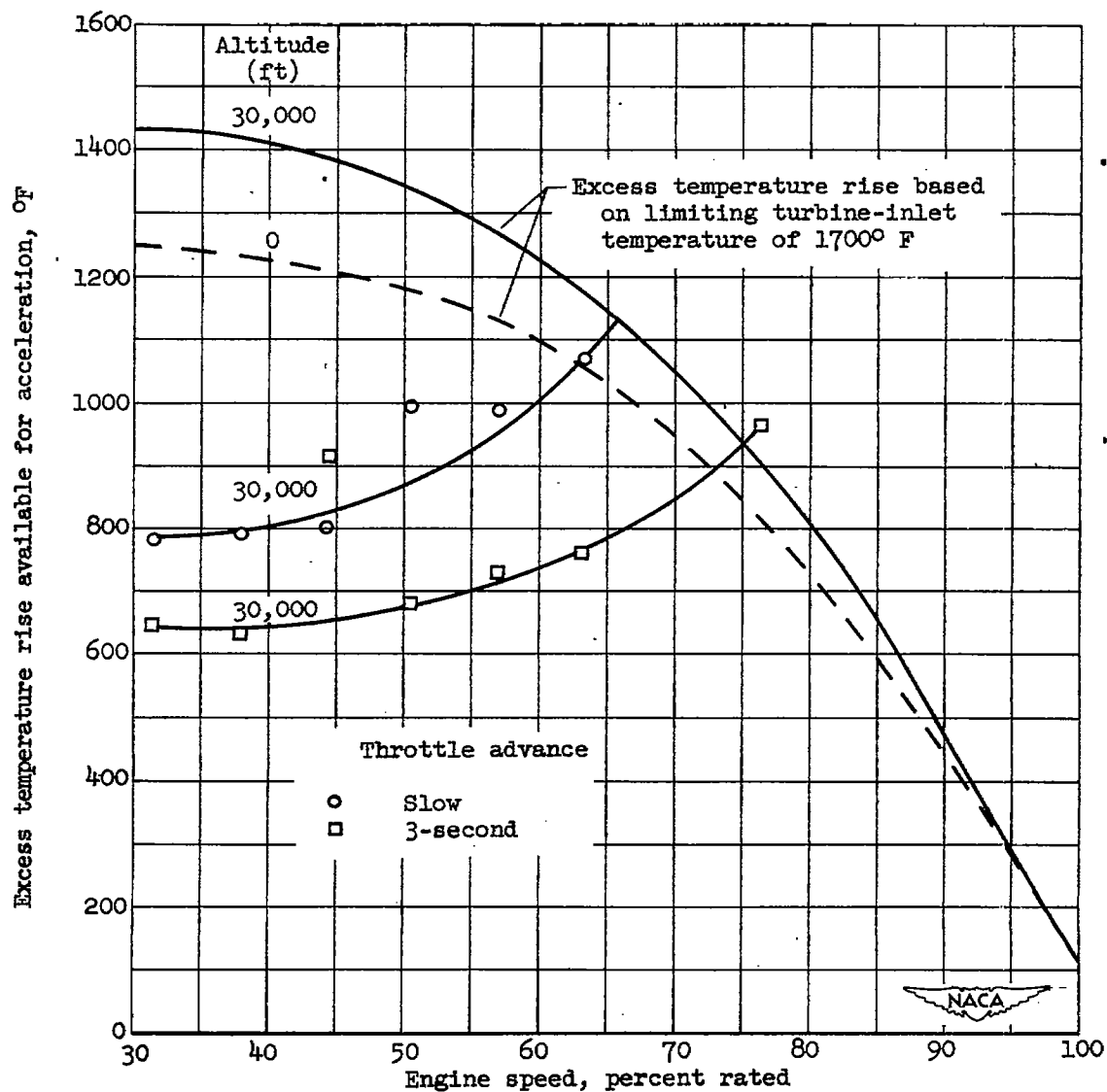


Figure 9. - Excess temperature rise available for engine acceleration: maximum obtainable temperature rise ( $\Delta T_{\max}$ ) minus temperature rise required for operation ( $\Delta T_{\text{req}}$ ). J47 single combustor; fuel, MIL-F-5572, grade 115/145 (weathered); flight Mach number, 0.52.

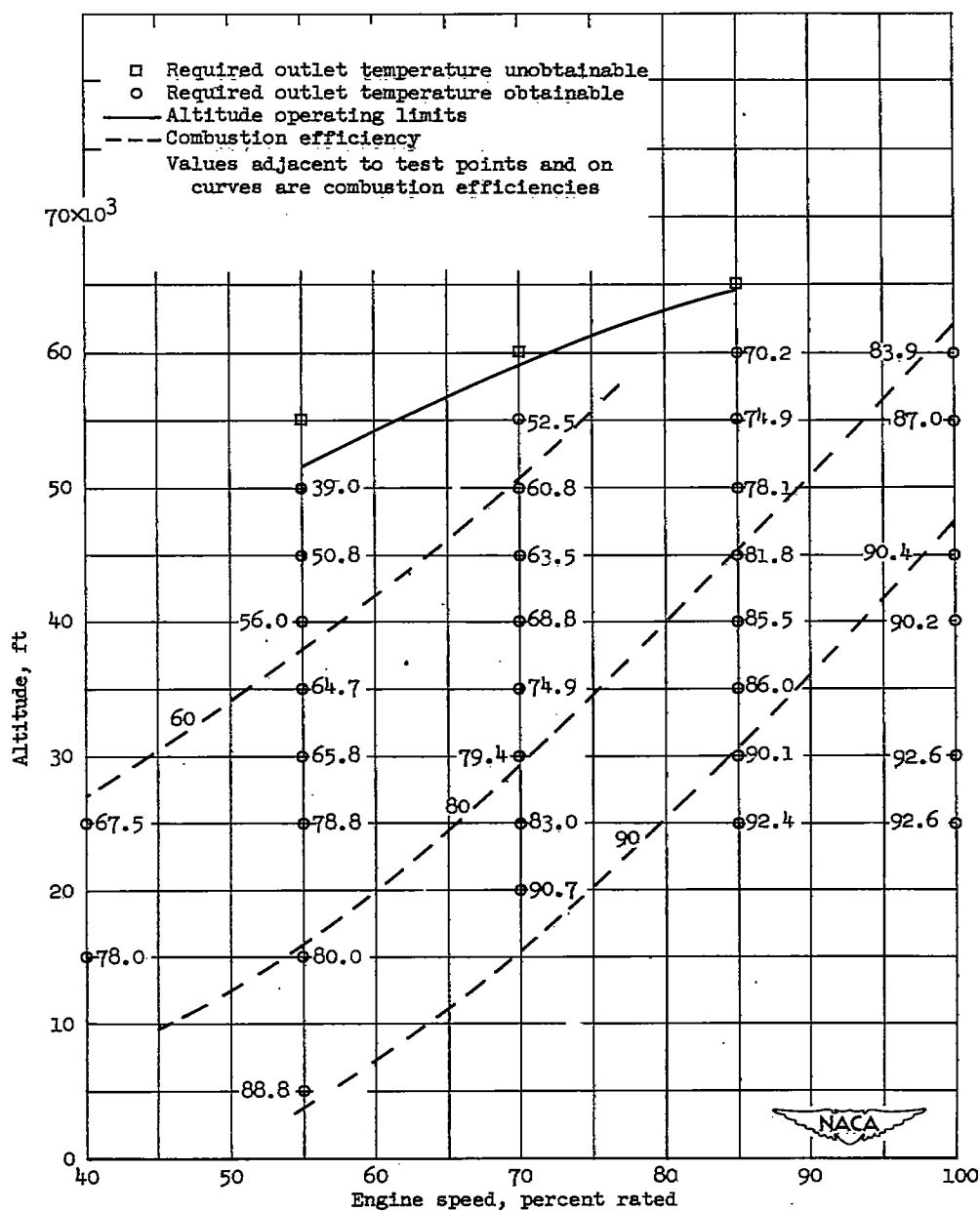


Figure 10. - Combustion efficiencies and altitude operating limits of J47 single combustor at various engine speeds and altitudes. Fuel, MIL-F-5572, grade 115/145 (weathered); flight Mach number, 0.52.

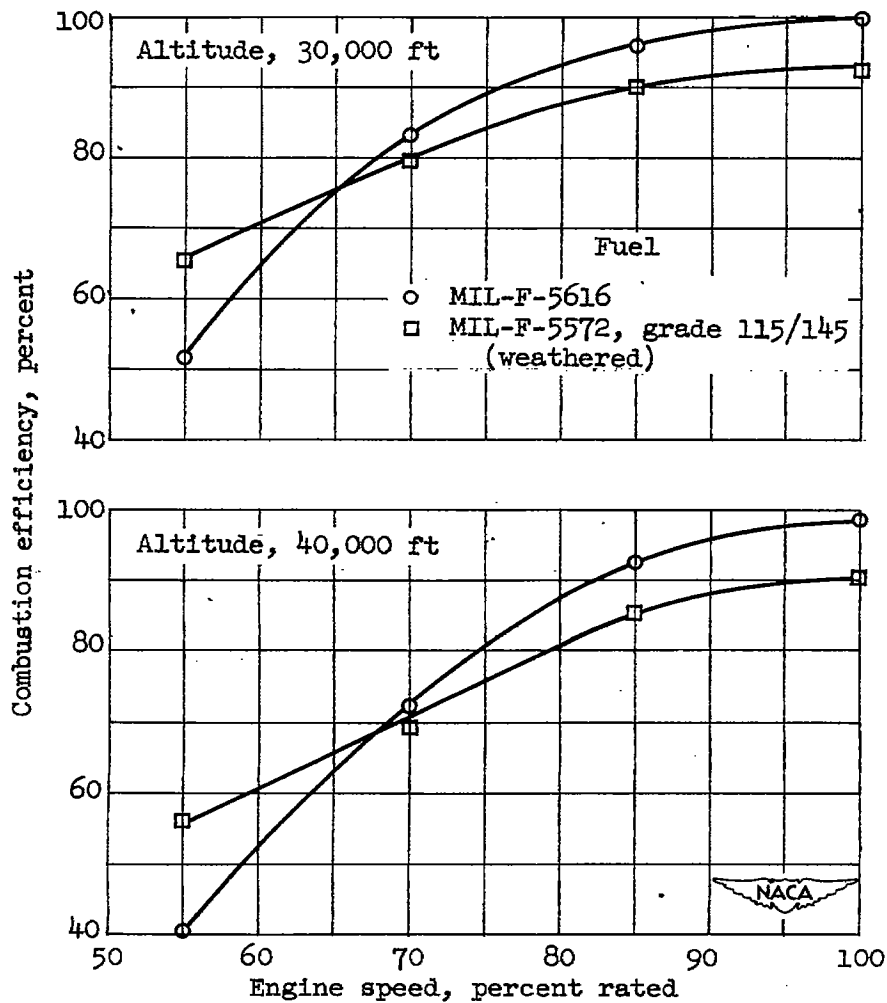


Figure 11. - Combustion efficiency of J47 single combustor with MIL-F-5616 and MIL-F-5572, grade 115/145 (weathered) fuels at 30,000- and 40,000-foot altitudes and various engine speeds. Flight Mach number, 0.52.

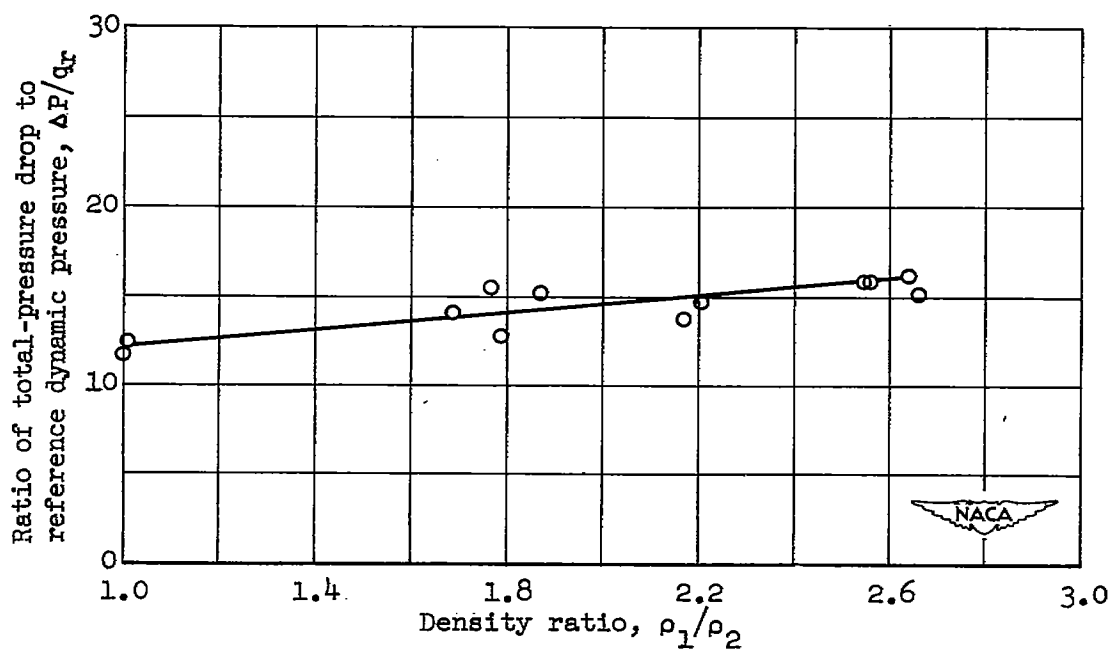


Figure 12. - Total-pressure drop across J47 single combustor.

NASA Technical Library



3 1176 01435 2224